Original Research

Synthesis and Photovoltaic Performance Evaluation of A Photo-Detector Prepared via Pulsed Laser Ablation

Raghad R. Mahdi [1], Ahmed N. Abd [2,*], Mohammed J. Mohammed Ali [2]

[1] Energy and Renewable Energies Technology Center, University of Technology-Iraq, Baghdad 10066, Iraq;
[2] Physics Department, College of Science, Mustansiriyah University, Baghdad 10052, Iraq
* Correspondence: ahmed_naji_abd@yahoo.com

Received: November 9, 2025; Accepted: January 30, 2026

Abstract: Pulsed laser ablation in liquid was used to prepare cadmium oxide (CdO) nanoparticles, providing a clean, path-selective process for building high-purity nanostructures with highly uniform morphology. The morphology and structure of the synthesised CdO nanoparticles were determined by XRD, and AFM. The polycrystalline cubic rock-salt structure with an average crystallite size of about 20 nm was confirmed by XRD. The spherical, cluster-like, cubic assembly of the nanocomposites was confirmed by SEM, and the uniform, smooth thin-film surface was examined by AFM. Optical studies revealed strong UV absorption with a peak at 340 nm, and the estimated optical band gap was 2.7 eV. A photo-detector was created by depositing CdO on porous silicon, which showed a wavelength-dependent photoresponse, with enhanced responsivity in the near-infrared region, achieving a maximum detectivity of 3.0×10^7 Jones at 950 nm. Additional FTIR and PL spectroscopy were performed for complementary chemical and luminescence characterisation. The findings demonstrate the potential of laser-synthesised CdO as a candidate material for plasmonic-compatible optoelectronic devices, especially for photodetection and NIR applications.

Keywords: cadmium oxide (CdO); porous silicon; pulsed laser ablation; photo-detector; quantum efficiency; specific detectivity

1. Introduction

In recent years, cadmium oxide (CdO) has attracted attention as a promising material for high-performance optoelectronic and photonic devices due to its distinctive, tunable structural, electrical, and optical properties. As an II-VI compound semiconductor, CdO is an excellent material for several optoelectronic applications due to its high density, approximately 8150 kg/m^3, tunable direct band gap energy ranging from 2.1 to 2.8 eV, depending on its synthesis condition, and remarkable electrical conductivity that can be further increased by intrinsic or extrinsic doping methods [1–4]. In addition, its high visible transmittance and good infrared reflectance make it a promising transparent conductive oxide (TCO) for solar cells, photo-detectors, and gas-sensing devices [5,6]. Because of their potential to improve the performance of optoelectronic devices, nanostructures are proving to be a powerful means of designing nanoscale materials.

Nanomaterials, materials with at least one dimension in the range of 1 to 100 nm, have size-dependent physicochemical properties due to various factors, including modified band structures, increased surface/volume ratios, and quantum confinement effects [7,8]. These properties enable enhanced light absorption, efficient charge-carrier generation, and fast response in photo-detectors.

Pulsed laser ablation in liquid (PLAL) has emerged as an attractive, clean, surfactant-free and controllable nanofabrication technique for the synthesis of high-purity semiconductor

nanoparticles. This approach ensures well-controlled tuning of particle size, morphology, and crystallinity, which are important for fully exploiting device performance [9,10]. Here, CdO nanoparticles were successfully prepared by PLAL, and a photo-detector was fabricated using them on porous silicon (P-Si). This could lead to a new generation of photo-detectors based on nano-CdO technology; this new device has potential applications in photonic systems, renewable energy, and future near-infrared detection. The morphology, structure, optical, and photoresponse properties of the prepared sample are systematically studied to determine whether it is a novel candidate material for future optoelectronic applications.

2. Experimental work

Cadmium oxide (CdO) nanoparticles were prepared using PLAL. Briefly, 10 g of commercially available CdO powder was ground by a high-energy ball mill, and the milled powder was passed through a 38-μm mesh to obtain a homogeneous particle size distribution. After that, the powder was pressed into a pellet at 8 MPa for 15 min using a hydraulic press to prepare a CdO target. The pellet was placed in 60 mL of deionised distilled water (DDW) and was pulsed laser-ablated using a Q-switched Nd:YAG laser with a wavelength of 1064 nm, a pulse laser flunce 2.92 J/cm^2, and 200 laser pulses. Upon irradiation, the nanoparticle-water solution turned a visible colour, indicating the formation of CdO nanoparticles and structural changes resulting from laser fragmentation and nucleation.

The P-Si substrate was formed with electrochemical etching. A p-type (100)-oriented silicon wafer (1.5 × 1 cm^2, resistivity ~1–5 Ω·cm) was cleaned using the RCA protocol to remove organic and metal impurities. The wafer was subsequently anodised in a room-temperature hydrofluoric acid (HF)/ethanol solution (40% HF and 99.99% ethanol) with a current density of 18 mA/cm^2 for 15 min. The resulting homogeneous porous layer exhibited a more well-defined pore morphology and a larger surface area than a smooth one, making it more suitable for nanoparticle deposition.

The drop-casting technique was used to deposit CdO nanoparticles onto the porous silicon substrates. The desired amount of the colloidal suspension of CdO was added dropwise (4 drops, ~10 μL each) using a micropipette (Model YE3K061872:10-1ML) and left at room temperature to dry, ensuring uniform adhesion to the porous surface. By depositing aluminium (Al) contacts on the front (CdO) and back surfaces (Si substrate) of the device using thermal evaporation, an Al/CdO/P-Si/Al heterojunction photo-detector with ohmic behaviour was fabricated. The upper Al electrode was patterned to provide an optical path to the active region.

X-ray diffraction (XRD) data of the grown CdO film were obtained using a Shimadzu XRD-6000 diffractometer (Cu Kα radiation, λ = 1.5406 Å). The samples were analysed by FT-IR absorption spectroscopy (ATR-diamond technique) using Digilab Excalibur FTS 3000MX spectrometer in the range 4000 to 600 cm^{-1}, resolution of 4 cm^{-1} and as much as 60 Co-added scans for obtaining information on different types of bonding in the structures and Photoluminescence (PL) is an important physical phenomena used to characterize semiconductors it depicts samples energy structure to reveal other important material features. The transition energy of the porus silicon is measured using (ELICO, SL174, SPECTROFLUORO-METER, Xe LAMP POWER SUPPLY). The mean crystallite size (D), dislocation density (δ), and microstrain (ε) were inferred from established models, as demonstrated in our previous study [11]. Optical properties were characterised using a Shimadzu UV-1800 spectrophotometer over a wavelength range of 300–1100 nm. The absorption and transmittance spectra of CdO thin films on the quartz substrates were measured for the calculation of the optical band gap (Eg), extinction coefficient (k), and optical conductivity (σ) using Tauc's relationship and classical optical formulae [8]. Finally, the major photo-detector performance parameters, that is, responsivity, specific detectivity (D*), quantum efficiency (QE), and spectral response, were estimated from the measured current-voltage (I-V) characteristics under illumination with light at different wavelengths.

3. Results and discussion

The XRD of crystalline silicon (c-Si) and porous silicon (P-Si) were collected. The profile of the c-Si peak is more intense and broader in the P-Si sample than in the bulk sample, as shown in Figure 1. This broadening is ascribed to effects from the nanocrystals formed on the pore walls during the electrochemical etching. The small shift of the P-Si peak towards smaller diffraction angles implies that the crystalline structure is maintained, while a slight lattice distortion is induced during the electrochemical etching process [12]. The structural parameters obtained from the XRD are listed in Table 1. The diffraction peak of the P-Si sample has a *d*-hkl value of 1.73 Å and is centred at 2θ = 69.66°. The average crystallite size ($D = 0.9\lambda/(\text{FWHM} \cos \theta)$, determined to be around
61.18 nm using the FWHM of 0.17°, indicates that the porous layer is nanocrystalline, this is in accordance with the international standard (JCPDS card Nos. 01-079-0613 and 00-027-1402). With a lattice constant of 1.234 nm and an estimated microstrain of 34.2 × 10^{-3}, it is evident that the development of pores in the silicon matrix causes internal stress. These results confirm that electrochemical etching (ECE) successfully yields nanostructured porous silicon layers without compromising the crystalline integrity, a critical requirement for optoelectronic applications where maximised surface area and charge-transporting properties are desired.

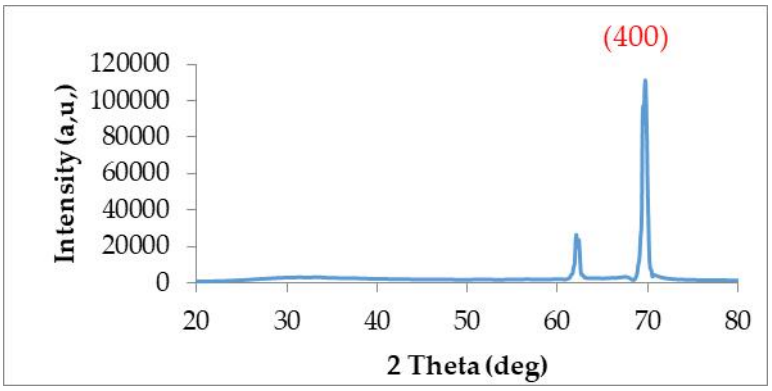

Figure 1. XRD patterns of P-Si.

Table 1. XRD parameters of the P-Si.

Samples	2θ(deg)	d(A)	FWHN (deg)	D(nm)	Lattice constant (nm)	Strain × 10^{-3} (lines^{-2}.m^{-4})
P-Si	69.66	1.73	0.17	61.18	1.73	34.2

The XRD patterns of the produced CdO thin film on a quartz substrate are displayed in Figure 2. The (002) and (111) crystallographic planes of CdO are identified by two prominent peaks in the XRD pattern located at 31.17° and 38.75°, respectively. No other peaks attributable to cubic phases or secondary impurities are observed, suggesting that the fabricated film has excellent phase purity. The (002) peak agrees with the standard reference pattern of cadmium oxide (JCPDS card No. 00-005-0640), indicating its preferential orientation and crystalline phase of the CdO pour structure. The absence of peaks is due to several reasons, the most important of which are: Weak crystallization or amorphous crystallinity, low concentration of crystalline material, and very, very small particle size. Table 2 provides a summary of the structural properties of the CdO thin film, including strain, lattice constants, and crystallite size.

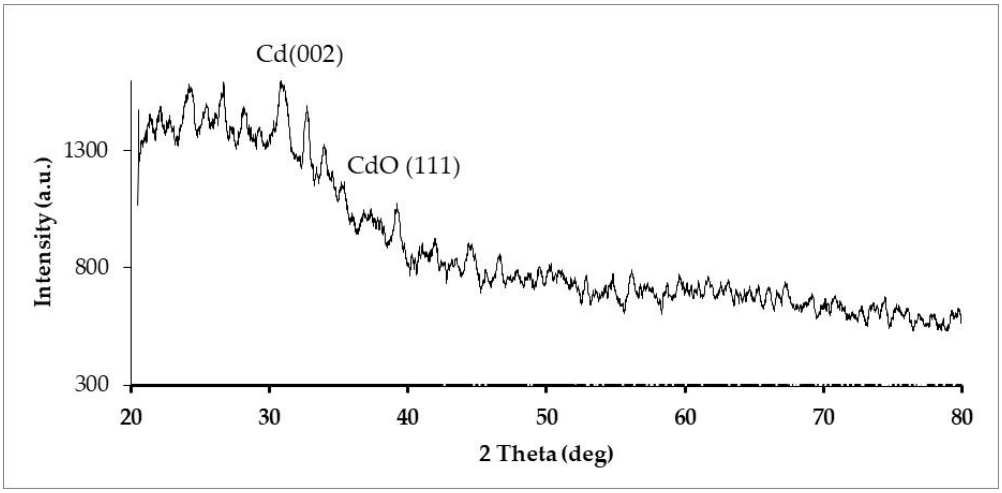

Figure 2. XRD pattern of synthesized CdO thin film.

Table 2. XRD parameters of CdO thin film.

2θ(deg)	hkl(plane)	d observed (Å)	d STEM	FWHM (deg)	D (nm)	$\delta \times 10^{14}$ *lines.m*$^{-2}$	$\eta \times 10^{-4}$ *lines*$^{-2}$.*m*$^{-4}$
31.17	(002)	5.67	5.5	0.41	20.51	23.76	16.89
38.75	(111)	4.59	4.5	0.52	16.75	35.60	20.67

The absorption spectrum of the CdO thin film is presented in Figure 3(a). The absorption increases with increasing wavelength, reaching a maximum at 340 nm, in the ultraviolet part of the spectrum. Beyond this, the absorbance decreases rapidly to a minimum at about 500 nm, then decreases slowly as the wavelength increases further. This broad absorption, extending from the near-UV to the visible range, makes CdO a promising candidate for use in Si/P-Si solar cells to enhance overall light absorption, extend the spectral response, and improve device efficiency [13,14]. By extrapolating the linear portion of the $(\alpha h\upsilon)^2$ vs photon energy ($h\upsilon$) plot for a direct allowed transition, the Tauc method was used to determine the optical energy band gap (Eg) when $\alpha = (2.303 \times A)/t$ and t (0.9 μm) represents the thickness of the CdO thin film, which was calculated using the gravimetric method [8]. At thickness = (0.9 μm), the CdO film produced in this study has a constant Eg of 2.7 eV, as shown in Figure 3(b). This value is comparable to those reported in the literature for CdO thin films, suggesting that the material developed has high optical quality [15].

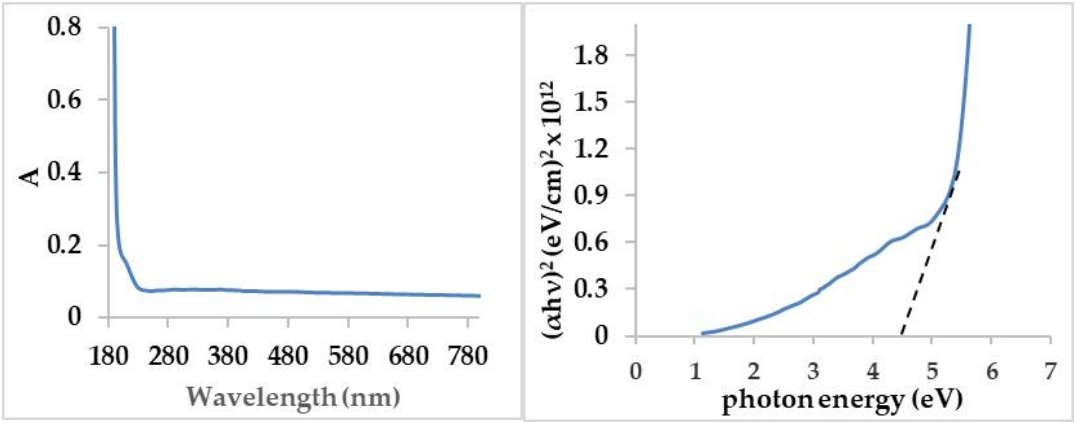

Figure 3. Optical properties of CdO thin films. (a) Absorption spectrum of CdO thin film; (b) Eg of CdO thin film.

The photoluminescence (PL) spectrum of the CdO sample is shown in Figure 4. The photon energy is 4.4 eV, this value is greater than the 2.7 eV optical band gap estimated from UV-Visible spectroscopy. This difference can be explained by considering the differences between these measurements. UV-Visible spectroscopy quantifies the absorption edge associated with the promotion of electrons from the valence band to the conduction band, which corresponds to the fundamental band gap. In comparison, PL spectroscopy registers information about the energy of photons emitted through the radiative recombination of the electron-hole (e-h) pairs, which typically occurs through defect states or lower-energy transitions within the band gap. Consequently, the energy of the emitted photon is usually less than the energy at which absorption has occurred, producing a lower apparent band gap in PL observations [16].

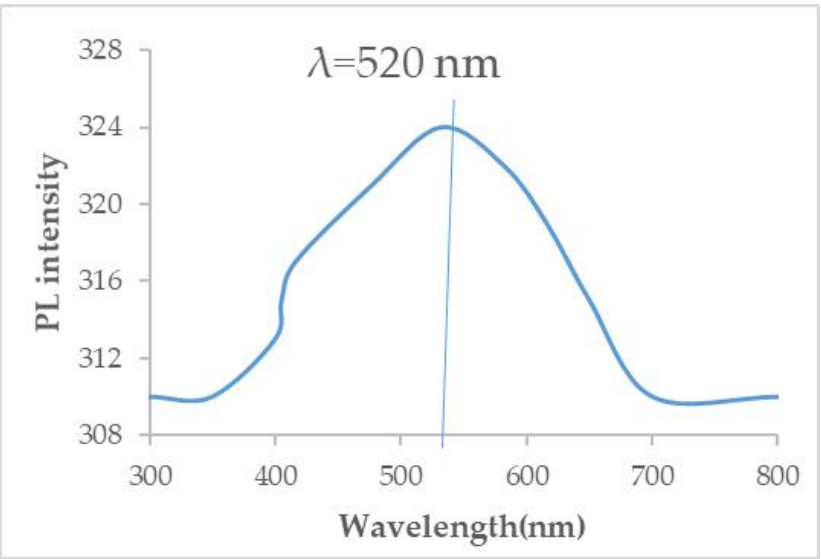

Figure 4. PL spectrum of the CdO thin film.

The FTIR spectrum of the prepared CdO sample is shown in Figure 5. Some characteristic vibrational bands are observed, indicating the existence of CdO phases and their chemical environment. Metal oxygen (M-O) stretching vibrations confirm the presence of CdO: This vibration appears as a prominent band at 1200 cm^{-1}. Accordingly, the O-H stretching vibrations of the water molecules physically adsorbed and chemically adsorbed on the surface and the hydroxyl (OH) groups bonded with cadmium are indicated by a wide absorbance band at 3421 cm^{-1}. Such a band is representative of surface hydration on the M-O nanostructures. The -O-C stretching vibration mode of acetyl groups, assigned to residual precursor background or surface-adsorbed species during the synthesis process, appears as a sharp peak at 1087 cm^{-1}. The band at 1399 cm^{-1}, which is assigned to the bending and wagging modes of CH_2 groups, suggests the presence of organic residues or capping agents. The nano-sized CdO appears to be incorporated in the host, giving rise to new absorption features in the spectrum. The increased intensity of the band at 1031 cm^{-1} and the slight changes in the intensity of the band at 1630 cm^{-1} due to Cd-O stretching vibrations confirm that the CdO is integrated inside the matrix. The bending vibration of adsorbed water molecules is also associated with this peak, and changes in this peak indicate the interaction of the CdO nanoparticles with an oxygen-rich environment. The FTIR spectral analysis presented here thus substantiates the presence of nanostructured CdO and indicates the impact of nanoscale effects on the vibrational modes of the material.

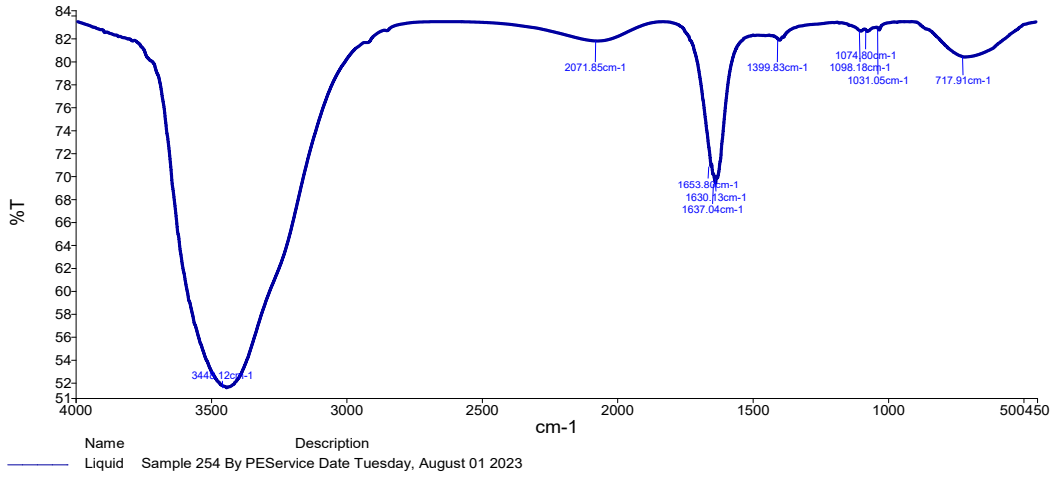

Figure 5. FTIR spectrum of CdO thin film.

The FTIR spectrum of porous silicon (P-Si) is shown in Figure 6. Characteristic absorption bands appeared in the spectrum, indicating that, due to the electrochemical etching process, a porous structure was formed, as well as the presence of surface functional groups. The broad absorption band at 1000–1500 cm^{-1}, with a maximum at 1600 cm^{-1}, is assigned to Si-H stretching and bending vibrations, suggesting that hydrogen-terminated silicon bonds are present at the pore surfaces. This hydrogen passivation of dangling bonds is a characteristic of newly prepared porous silicon and enhances structural stability. A strong peak at 2857 cm^{-1} in the 2500–3500 cm^{-1} region may be connected to the C-H stretching vibrations attributed to hydrocarbon contaminants or organic residues from previous steps in the etching solution (such as the use of ethanol). Additionally, a wide band from 3428 to 3766 cm^{-1} is due to the O-H stretching vibrations of the adsorbed water molecules and surface hydroxyl (OH) groups. This demonstrates that the increased surface area of the nanostructure pores leads to partial surface oxidation of the porous silicon layer when the sample is exposed to ambient air. The FTIR spectral results presented in this work confirm the successful generation of porous silicon and emphasise that the roles of hydrogen, carbon, and oxygen surface species can differ substantially in controlling the chemical and electronic properties of porous silicon.

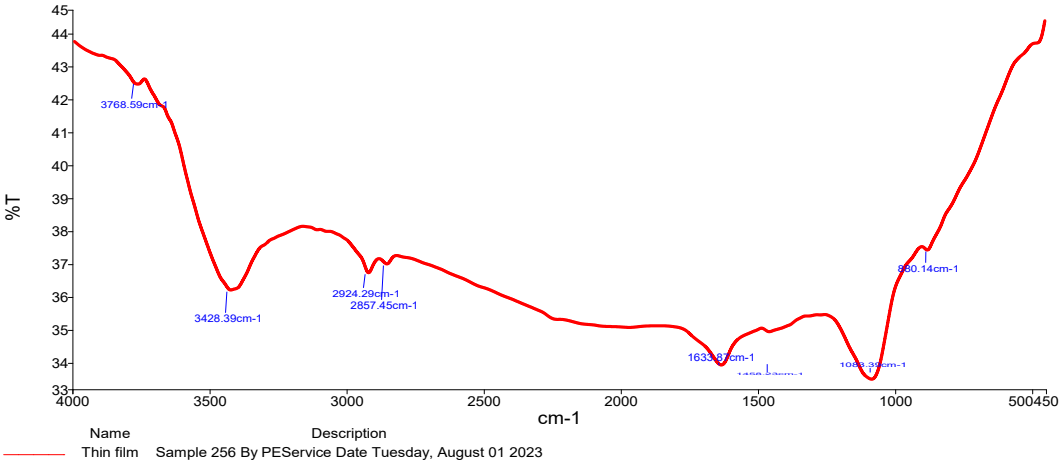

Figure 6. FTIR spectrum of porous silicon (P-Si) layer.

Figure 7 shows the surface morphology of the CdO thin film. The crystals are uniformly distributed with well-defined borders, and the film has a very compact structure. The grains are interconnected, with no voids or pores: This is a very homogeneous, continuous film of very good

crystalline quality. This morphology is conducive to the efficient charge transport and good inter-grain percolation relevant to optoelectronic applications.

In contrast, the P-Si surface has a uniform pattern of round pores separated by nanoscale walls. The pore distribution is regular, indicating a uniform porous structure with well-defined morphology, which promotes light trapping and increases the device-integration surface area. The morphological details of CdO and P-Si in terms of surface roughness, grain size, and porosity are given in Table 3.

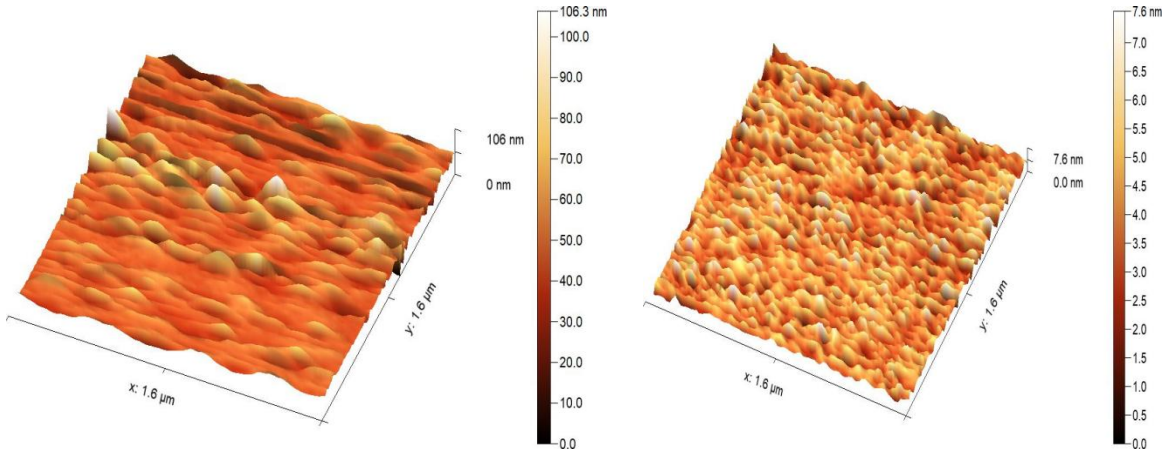

Figure 7. AFM images of CdO thin film.

Table 3. AFM morphological parameters of the CdO and (P-Si) thin films.

Samples	Average grain size (nm)	Root mean square (nm)	Roughness average (nm)
CdO	7.20	1.24	0.96
P-Si	63.82	9.03	5.87

Figure 8 shows the spectrum responsivity of a photo-detector based on CdO nanoparticles as a function of wavelength, ranging from 350 to 1000 nm. Using a Nd:YAG laser (λ = 1064 nm) with a pulse energy of 480 mJ and a repetition rate of 8 Hz, simple CdO nanoparticles were created by PLAL (water). Electrochemical etching for 15 min at a current density of 18 mA/cm^2 was used to create P-Si substrates. The spectral curve shows three obvious extrema. The initial peak (450 nm) is related to the intrinsic photoresponse of CdO nanoparticles, suggesting efficient absorption in the visible region, as well as excellent carrier generation. The near-IR (NIR) response of the PS substrate is responsible for the third, dominant peak at 980 nm, while the second peak at 800 nm is attributed to the band-edge absorption of Si. Significantly, an obvious increase in responsivity at the 980 nm peak indicates improved light absorption and more effective charge separation in the NIR region. This enhancement is presumably due to the synergistic effects of the nanoscale morphology of CdO, the light-trapping properties of the porous silicon structure, and potential interfacial energy transfer. The robust NIR response indicates that the Al/CdO/P-Si/Al is very promising for high-performance photodetection over the visible and NIR ranges.

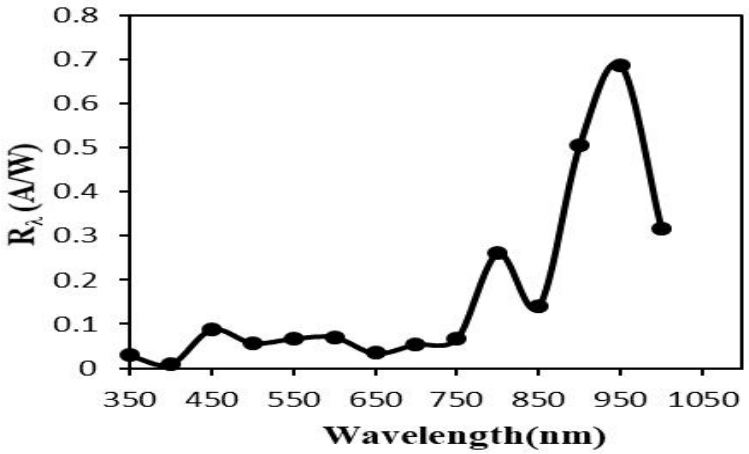

Figure 8. Spectral responsivity of CdO-based photo-detector as a function of wavelength.

The specific detection (D*) was simulated as a function of the wavelength using the spectral responsivity to assess the performance and suitability of the fabricated photo-detector. As shown in Figure 9, the detector can achieve a maximum specific detectivity of 3.0×10^7 Jones (3.0 × 106 Jones) at 950 nm. The high detectivity value implies excellent sensitivity and low noise, further demonstrating the potential of this device for effective NIR photodetection.

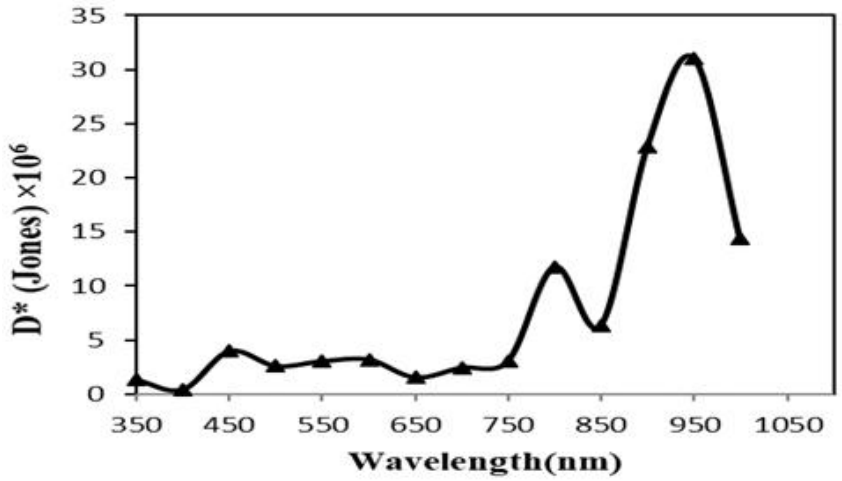

Figure 9. Specific detection of CdO-based photo-detector as a function of wavelength.

To investigate the improved performance of the prepared detector, the quantitative efficiency ($EQE\% = R_\lambda \frac{1.24}{\lambda_{(\mu m)}} \times 100\%$) was estimated. As seen in Figure 10, the improvement is due to the widespread increase in the absorption of electromagnetic radiation in the visible to NIR region. This is due to the increased number of layers in the detector, which decreases the voltage barrier, lowers the energy demand, facilitates charge transfer to the maximum and minimum wavelengths, and increases the number of charge carriers. These layers also include materials and silicon that enhance the absorption of rays and reduce their reflection.

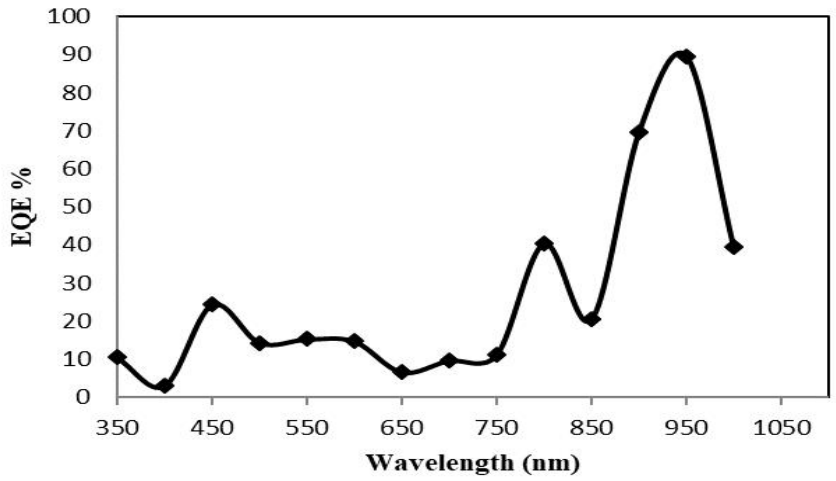

Figure 10. External quantum efficiency (EQE) of CdO photo-detector as a function of wavelength.

4. Conclusions

In this work, CdO nanoparticles were prepared using pulsed laser ablation and porous silicon (P-Si) was prepared by electrochemical etching. Structural and morphological characterisations established the quality of the synthesised materials. AFM analysis showed the thin film had a smooth, homogeneous surface with very good crystalline regularity. XRD showed that the CdO nanostructure was a single-phase crystalline material and confirmed its crystallinity. The optical absorption spectrum showed intense absorbance in the UV-visible domain (300–500 nm) and an estimated direct Eg of about 2.7 eV, typical of CdO. These optoelectronic properties make the material promising for applications in optoelectronic devices, such as photo-detectors. The solar cell performance of the devices was analysed using key photovoltaic performance parameters: QE, specific detectivity, and spectral response. The responses were large in the visible and NIR regions, and the maximum detectivity reached 3.0×10^7 Jones at 950 nm, originating from QE enhanced by improved light absorption, downshifted potential barrier, and effective charge-carrier generation. Overall, the prepared CdO/P-Si photo-detector exhibits excellent structural, optical, and photoresponse properties, indicating its promise for high-performance optoelectronic and photonic devices.

Acknowledgments: The authors gratefully acknowledge the anonymous peer reviewers for their insightful comments and constructive feedback, which significantly contributed to the enhancement of this manuscript's quality.

Availability of Data and Materials: The datasets used and analyzed during the current study are available from the corresponding author on reasonable request.

Funding: This research received no external funding.

Author Contributions: RRM, ANA, and MJMA conceived and designed the research framework; RRM and ANA carried out the experimental and computational work; ANA and MJMA provided critical guidance on the analytical methods and interpretation of results; MJMA performed the data analysis; ANA prepared the initial draft of the manuscript. All authors have read and approved the final manuscript. All authors contributed to editorial changes in the manuscript. All authors have participated sufficiently in the work and agreed to be accountable for all aspects of the work.

Conflicts of Interest: The authors declare no conflict of interest.

References

1. Spencer, J.A.; Mock, A.L.; Jacobs, A.G.; et al. A review of band structure and material properties of transparent conducting and semiconducting oxides: Ga_2O_3, Al_2O_3, In_2O_3, ZnO, SnO_2, CdO, NiO, CuO, and Sc_2O_3. *Applied Physics Reviews* 2022, 9(1), 011315. https://doi.org/10.1063/5.0078037
2. Abd, A.N.**;** Al-Marjani, M.F.; Kadham, Z.A. Synthesis of CdO NP S for antimicrobial activity. *International Journal of Thin Film Science and Technology* 2018, 7(1), 43–47. https://doi.org/10.18576/ijtfst/070106
3. Nolen, J.R.; Runnerstrom, E.L.; Kelley, K.P.; et al. Ultraviolet to far-infrared dielectric function of *n*-doped cadmium oxide thin films. *Physical Review Materials* 2020, 4(2), 025202. https://doi.org/10.1103/PhysRevMaterials.4.025202
4. Habubi, N.F.; Abd, A.N.; Ismail, R.A.; et al. Improved photoresponse of porous silicon photodetectors by embedding CdSe nanoparticles. *Indian Journal of Pure and Applied Physics* 2015, 53(11), 718–724. https://inis.iaea.org/records/ey0eq-qrz23
5. Jlassi, M.; Ben Miled, I.; Sta, I.; et al. Fabrication and Characterization of Nanostructured Cadmium Oxide Thin Films Doped with Indium by Sol-Gel Spin-Coating for CdO (n)/Si (p) Heterojunction Photodiode Applications. *Silicon* 2025, 17, 3033–3044. https://doi.org/10.1007/s12633-025-03391-8
6. Salim, E.T.; Ismail, R.A.; Fakhri, M.A.; et al. Synthesis of Cadmium Oxide/Si Heterostructure for Two-Band Sensor Application. *Iranian Journal of Science and Technology, Transactions A: Science* 2019, 43(3), 1337–1343. https://doi.org/10.1007/s40995-018-0607-8
7. Azam, Z.; Ayaz, A.; Younas, M.; et al. Microbial synthesized cadmium oxide nanoparticles induce oxidative stress and protein leakage in bacterial cells. *Microbial Pathogenesis* 2020, 144, 104188. https://doi.org/10.1016/j.micpath.2020.104188
8. Ali, A.A.H.; Noor, H.A.; Hussain, S.A. Study of the effect of non-thermal plasma on the structural properties of pure Cadmium Oxide thin Films (CdO) prepared by Pulsed laser Deposition Technique (PLD). *Journal of Kufa-Physics* 2019, 11(1), 63–70. https://doi.org/10.31257/2018/jkp/2019/110108
9. Ali, M.J.M.; Hassan, H.R.; Abd, A.N. Preparation and Characterization of Ag/CdTeQDs/PS/c-Si/Ag Heterojunction for Photodetector Applications. In: *Proceedings of the 5th International Specialized Conference of Education College on Physics and Applied Sciences* (5thICECAS24); April 22–23, 2024; Baghdad, Iraq. 605–610.
10. Ali, M.J.M.; Abdulkhaleq, N.A.; Hamza, B.H.; et al. Innovative FeS@Se nanostructures via pulsed laser ablation to enhance the heterojunction performance of FeS/Si photodetectors. *Applied Nanoscience* 2025, 15(4), 30. https://doi.org/10.1007/s13204-025-03103-z
11. Aziz, S.A.; Ali, R.S.; Abd, A.N. Characterization studies of nickel oxide nanostructure films prepared by electrolysis method for photo detectors applications. *NeuroQuantology* 2020, 18, 45–49. https://doi.org/10.14704/nq.2020.18.2.NQ20123
12. Abood, M.K.; Wahid, M.H.A.; Salim, E.T.; et al. Niobium Pentoxide thin films employ simple colloidal suspension at low preparation temperature. In *Proceedings of the International Conference on Applied Photonics and Electronics 2017* (InCAPE2017); 9–10 August 2017; Port Dickson, Malaysia. pp. 01058.
13. Moniruzzaman, S.; Teresa, J.; Carlissa, F.; et al. Sol-Gel Derived CdO:Al Thin Films on Various Substrates: A Comprehensive Study on Structural, Morphological, Optical, and Electrical Properties. *Journal of Materials Science Research* 2025, 14(1). https://doi.org/10.5539/jmsr.v14n1p22
14. Upadhyay, G.K.; Kumar, V.; Purohit, L.P. Optimized CdO: TiO_2 nanocomposites for heterojunction solar cell applications. *Journal of Alloys and Compounds* 2021, 856, 157453. https://doi.org/doi.org/10.1016/j.jallcom.2020.157453
15. Karoui, R. Spectroscopic technique: *Modern Techniques for Food Authentication*, 2nd ed. Academic Press; 2018. pp. 219–252.
16. Prakash, T.; Kumar, R.E.; Neri, G.; et al. Evaluation of structural, morphological and optical properties of CdO nanostructures. *Ceramics International* 2022, 48, 1223–1229. https://doi.org/10.1016/j.ceramint.2021.09.207